

# An Esterase with Superior Activity and Enantioselectivity towards 1,2-*O*-Isopropylidenglycerol Esters Obtained by Protein Design

Luis F. Godinho,<sup>a</sup> Carlos R. Reis,<sup>a</sup> Ronald van Merkerk,<sup>a</sup> Gerrit J. Poelarends,<sup>a</sup> and Wim J. Quax<sup>a,\*</sup>

<sup>a</sup> Department of Pharmaceutical Biology, Groningen Research Institute of Pharmacy, University of Groningen, Antonius Deusinglaan 1, 9713 AV Groningen, The Netherlands  
Fax: (+31)-50-363-3000; phone: (+31)-50-363-7660; e-mail: w.j.quax@rug.nl

Received: March 14, 2012; Revised: July 5, 2012; Published online: November 4, 2012

Supporting information for this article is available on the WWW under <http://dx.doi.org/10.1002/adsc.201200211>.

**Abstract:** The *Escherichia coli* esterase YbF displays high activity towards 1,2-*O*-isopropylidenglycerol (IPG) butyrate and IPG caprylate, and prefers the *R*-enantiomer of these substrates, producing the *S*-enantiomer of the IPG product in excess. To improve the potential of the enzyme for the kinetic resolution of racemic esters of IPG, an enhancement of the activity and enantioselectivity would be highly desirable. Molecular docking of the *R*-enantiomer of both IPG esters into the active site of YbF allowed the identification of proximal YbF active site residues. Four residues (25, 124, 185 and 235) were selected as targets for mutagenesis, in order to enhance YbF activity and enantioselectivity towards IPG esters. Random mutagenesis at positions 25, 124, 185 and

235 yielded several best YbF variants with enhanced activity and enantioselectivity towards IPG esters. The best YbF mutant, W235I, exhibited a 2-fold higher enantioselectivity than wild-type YbF, with an  $E=38$  for IPG butyrate and an  $E=77$  for IPG caprylate. Molecular docking experiments further support the enhanced enantioselectivity shown experimentally and the structural effects of this amino acid substitution on the active site of YbF are provided. The engineered W235I mutant is an attractive catalyst for practical applications in the kinetic resolution of IPG esters.

**Keywords:** enantioselectivity; *Escherichia coli*; esterases; kinetic resolution; protein engineering

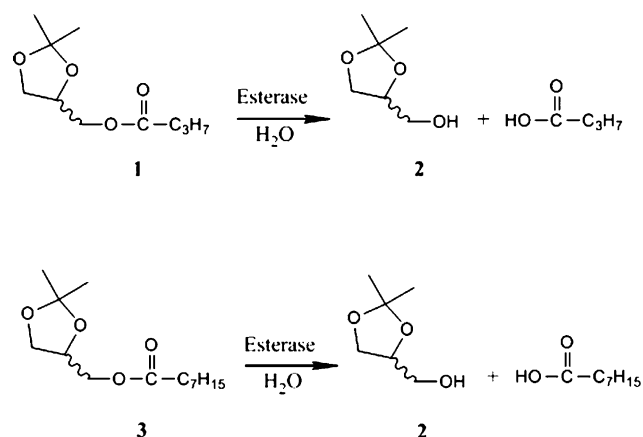
## Introduction

Esterases represent a class of hydrolytic enzymes that are highly useful for organic synthesis, as they have broad substrate specificity and exhibit often high stereoselectivity.<sup>[1,2]</sup> The development of an esterase-based biocatalytic process for the kinetic resolution of racemic 1,2-*O*-isopropylidenglycerol (IPG) esters (Scheme 1) has exciting potential for organic synthesis because the optically pure product (*S*)-IPG is an important building block for the preparation of  $\beta$ -blockers, prostaglandins, and leukotrienes.<sup>[3,4]</sup>

In an ideal case, the esterase converts only the *R*-enantiomer of the IPG ester, yielding the optically pure product (*S*)-IPG.

Previously, we have reported that the cytoplasmic esterase YbF from *Escherichia coli* has high hydrolytic activity and enantioselectivity towards IPG esters with different alkyl chains. YbF displays mod-

erate enantioselectivity ( $E=10$ ) towards IPG butyrate (**1**) and a high enantioselectivity ( $E=29$ ) towards IPG



**Scheme 1.** Esterase-catalyzed conversion of IPG esters.

caprylate (**3**).<sup>[5]</sup> The crystal structure of YbF has been solved and the enzyme is composed of an  $\alpha/\beta$  hydrolase-fold domain with a three-helical bundle cap that is linked by a twist helix to the  $\alpha/\beta$  hydrolase-fold domain.<sup>[6]</sup> The sequence motif GxSxG, characteristic for  $\alpha/\beta$  hydrolase-fold superfamily of enzymes, is also conserved in YbF. However, YbF has less than 20% sequence identity with most known esterases and likely to contain a catalytic tetrad of Ser89-His234-Asp113-Ser206 (with the first Ser being the nucleophile) instead of the conserved catalytic triad.<sup>[6]</sup> It was reported that the spatial position of the conserved catalytic Asp113 in YbF differs from the spatial position observed for the catalytic acid residue from other hydrolases, and that the Ser206 takes up the spatial position of the catalytic acid residue.<sup>[6]</sup> Evidence for a fourth catalytic residue such as Ser206 has also been obtained in other members of the hydrolase family.<sup>[7]</sup>

Although wild-type YbF exhibits significant activity and selectivity towards IPG esters, it still requires further improvement towards these substrates for practical applications. In the last two decades novel laboratory evolution methods have been devised in order to improve enzyme properties (such as activity, stability and selectivity) towards non-natural substrates.<sup>[8–10]</sup> Random evolution approaches have been the preferred method of choice, since they do not require detailed knowledge of the enzyme structure or reaction mechanism. However, with the increased number of 3D structures solved and the growth of computational methods, structure-based enzyme engineering strategies are becoming more in reach for improving enzyme properties. The major advantage of this structure-based approach is that it allows for the generation of smaller libraries, reducing the time of screening or selection, with higher functional diversity.<sup>[8–12]</sup>

Herein, we describe molecular docking experiments of (*R*)-**1** into the YbF active site in order to identify active site residues that are in close proximity to the substrate. These docking experiments helped to identify four positions (25, 124, 185 and 235) in the YbF active site that might be good targets for engineering the enantioselectivity of YbF towards **1** and **3**. These positions were randomized by site-saturation mutagenesis and four single-site libraries were created. We used activity screening (colorimetric screen) to select for YbF clones with improved enantioselectivity towards substrate **1**.<sup>[13]</sup> Several single mutants at positions 185 and 235 affected YbF enantioselectivity towards substrates **1** and **3**. The best mutant (W235I) showed significantly higher activity and enantioselectivity towards both substrates **1** and **3**, when compared to the wild-type enzyme. A possible mechanism is devised to explain the experimental observations obtained for the best YbF mutant.

## Results and Discussion

In previous work reported by our group,<sup>[5]</sup> YbF was identified as the major enzyme responsible for the pronounced activities and enantioselectivities in cell-free extracts prepared from *E. coli* cells toward substrates **1** and **3** (Scheme 1), with formation of (*S*)-**2** in excess over (*R*)-**2** for both substrates. YbF exhibits moderate enantioselectivity ( $E=10$ ) towards **1** and a high enantioselectivity ( $E=29$ ) towards **3**.<sup>[5]</sup> Based on previous molecular docking experiments, where the *R*-enantiomer of **1** or **3** was modeled into the active site of YbF, we obtained insight in the binding mode of these IPG esters. The docking model suggests that the short alkyl chain of substrate **1** can be accommodated in the thin hydrophobic pocket, while for substrate **3** the longer alkyl chain is accommodated along the crevice. These observations set the stage for the mutagenesis study reported here. A detailed examination of the most favorable binding poses of (*R*)-**1** and (*R*)-**3** in the active site of YbF (Figure 1), revealed several active site residues that are in close proximity to these substrates. Two residues (L25 and I185) that are part of the catalytic cavity were select-

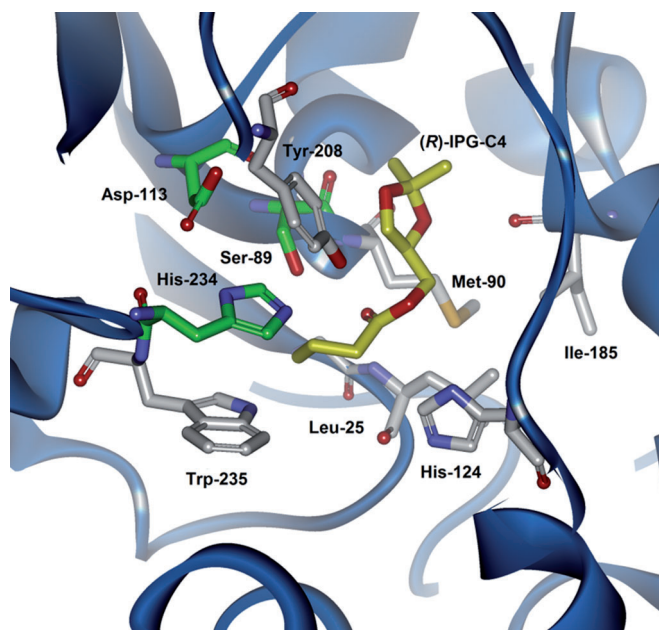


**Figure 1.** Close-up view of the catalytic residues (green sticks) and mutated active site surrounding residues of YbF (white sticks) in complex with the most favorable docked pose for (*R*)-IPG-C4 (*R*-1) (yellow sticks). The carbonyl oxygen of (*R*)-IPG-C4 is at hydrogen bonding distance to the nitrogen atoms of Leu-25 and Met-90, suggesting that these two residues compose the oxyanion hole of YbF and trap the carbonyl oxygen atom of the substrate, in agreement with the mechanism suggested for other hydrolases of this family.<sup>[5]</sup> Docking of substrate and minimization runs were performed using available tools in Discovery Studio 2.5.

ed for mutagenesis along with two aromatic residues (H124 and W235) that form the neck in the bottom region of the L-shaped sack (crevice).

### Library Construction and Activity Screening

To investigate the effect of different amino acid side chains at the four selected positions (L25, H124, I185 and W235) on YbF enantioselectivity, each selected residue was replaced by 12 other residues (Phe, Leu, Ile, Val, Cys, Arg, Ser, Gly, Tyr, His, Asn, Asp). Four single-site libraries were generated with the help of degenerate NDT primers, comprising 12 codon variants, with a balanced mix of aliphatic and aromatic, polar and non-polar, positively and negatively charged residues.<sup>[14]</sup> The resulting libraries were screened for clones that exhibited higher enantioselectivity towards **1**. The screening assay used was based on the colorimetric method developed by Janes et al.<sup>[13]</sup> Cells of the YbF clones from each library were first grown in deep-well plates, after which cells were washed, lysed and assayed separately for their ability to hydrolyse (*R*)-**1** and (*S*)-**1**. The clones initial rates of hydrolysis of (*R*)-**1** and (*S*)-**1**, were measured separately using a pH indicator (4-nitrophenol).<sup>[13]</sup> Overall, 27 out of 128 clones from the four libraries were pre-selected due to their apparent higher enantioselectivity towards **1**, when compared to wild-type YbF. Under the assay conditions used, no hydrolysis of **1** by the cell free extract (CFE) of *E. coli* BL21 (DE3) cells transformed with pET26b (an empty vector not harboring the YbF gene) was detected, implying that the activity of the YbF protein encoded by the endogenous chromosomal *ybfF* gene is not detectable.

Clones that exhibited apparent higher enantioselectivity towards **1** were selected for further analysis by chiral GC. The cells of the 27 selected clones were re-grown, cell free extract prepared, and each CFE incubated at 30 °C in the presence of **1**. Out of the 27 clones screened, five (two clones from library 185 and

three clones from library 235) of them were selected based on their apparent increased enantioselectivity towards substrate **1**. The plasmids from the five selected clones were isolated and the YbF mutant gene was sequenced. Sequence analysis revealed that both clones from library 185 contained the same mutation I185V, whereas the clones from library 235 contained the following mutations: W235V, W235I, and W235E.

These mutants and wild-type YbF were produced in the cytoplasm of *E. coli* BL21 (DE3) and purified to >90% homogeneity (as assessed by SDS/PAGE) using an Ni-based immobilized metal affinity chromatography procedure. The purification procedure used to purify YbF wild-type and mutants is highly specific for proteins containing a His-tag, so that the possibility of contamination from native YbF from the host organism is eliminated. The purified enzymes were stored at –80 °C until further use.

### Kinetic Resolution of IPG Esters

The activity and enantioselectivity of YbF wild-type and mutants toward substrates **1** and **3** were investigated by kinetic resolution experiments (Table 1). Mutant I185V exhibited higher activity and showed the same enantioselectivity ( $E=12$ ) towards substrate **1** when compared to YbF wild-type. For substrate **3**, the mutant I185V was also more active than wild-type YbF, however its enantioselectivity was reduced by 2-fold. Mutants W235V, W235I, and W235E displayed both higher activity and enantioselectivity towards substrate **1** when compared to wild-type YbF, with mutant W235I exhibiting the most pronounced enantioselectivity ( $E=38$ ). Similarly, for substrate **3** all mutants showed higher activity when compared to wild-type YbF, but only mutant W235I showed higher enantioselectivity ( $E=77$ ) than wild-type YbF.

To demonstrate the synthetic potential of mutant W235I for the preparation of (*S*)-IPG, the kinetic resolution of racemic **3** (5 mM) by YbF wild-type

**Table 1.** Results of kinetic resolution experiments with wild-type and mutants of YbF using substrates **1** or **3**.<sup>[a]</sup>

Enzyme	$ee_p$ [%] <sup>[b]</sup>	Substrate <b>1</b>			Substrate <b>3</b>			$E$
		$ee_s$ [%] <sup>[c]</sup>	C [%] <sup>[d]</sup>	$E$ <sup>[e]</sup>	$ee_s$ [%]	C [%]		
wild-type	76	57	43	12	92	52	36	40
I185V	69	76	52	12	83	64	44	20
W235I	88	79	47	38	95	66	41	77
W235V	77	80	51	18	84	82	49	30
W235E	77	89	54	22	88	74	46	34

<sup>[a]</sup> Kinetic resolution assays were performed in 70 mM MOPS buffer (pH 7.5) containing Tween 80 (14.3%, w/v) at 30 °C.

<sup>[b]</sup>  $ee_p$ : enantiomeric excess of product.

<sup>[c]</sup>  $ee_s$ : enantiomeric excess of substrate.

<sup>[d]</sup> C: substrate conversion.

<sup>[e]</sup>  $E$ : enzyme enantioselectivity, the five enzymes prefer the *R*-enantiomer of **1** and **3**, producing *S*-IPG.

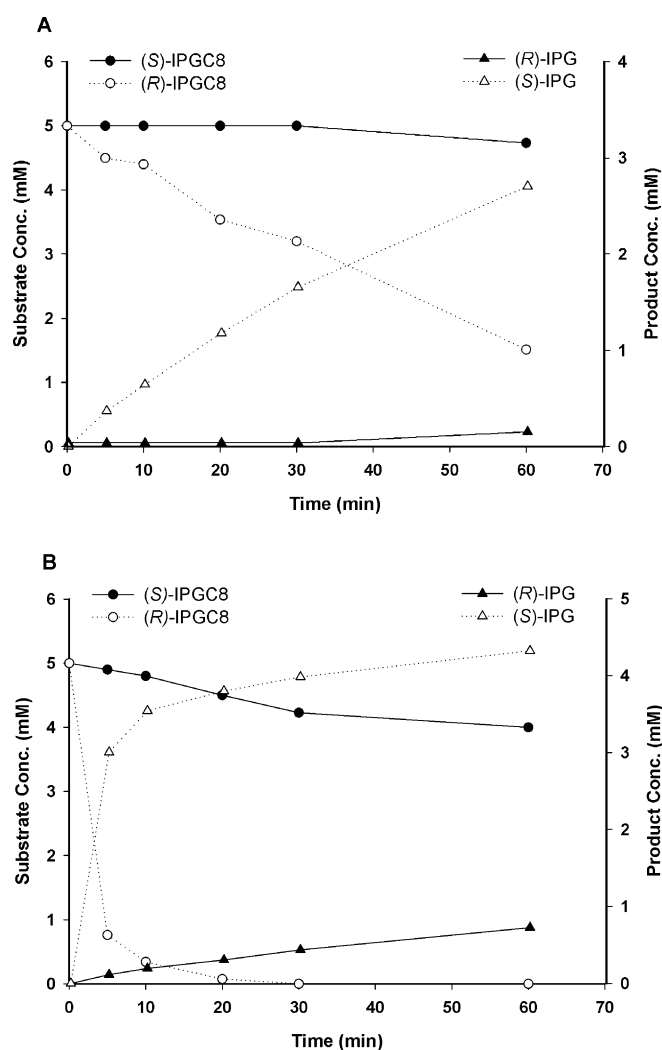


**Figure 2.** Kinetic resolution of 5 mM racemic IPG caprylate (**3**) with 0.3  $\mu\text{M}$  of YbfF wild-type (**A**) and with 0.3  $\mu\text{M}$  of mutant W235I (**B**). The substrates are represented by round symbols, where (●) represents the *S*-enantiomer and (○) represents the *R*-enantiomer. The products are represented by triangles, where (▲) represents the *R*-enantiomer and (△) represents the *S*-enantiomer.

(0.3  $\mu\text{M}$ ) and mutant W235I (0.3  $\mu\text{M}$ ) is demonstrated in Figure 2. After 10 min, the W235I mutant had reached 93% conversion of (*R*)-**3** while the wild-type showed only 12% conversion. For substrate (*S*)-**3**, the W235I mutant had reached 20% conversion after 60 min, while the wild-type showed only 6% conversion. Both YbfF wild-type and mutant showed high enantioselectivity in the formation of (*S*)-**2** (wild-type: 92% *ee*; W235I: 95% *ee*). Overall, the mutant showed a  $\sim 7.5$ -fold increase in the catalytic activity towards the *R*-substrate whereas for the *S*-substrate the increase was only  $\sim 3.3$ -fold, when compared to the wild-type enzyme. These results are in accordance with the data obtained from the kinetic parameters determined in the next section.

The effect of pH and temperature on enzyme activity (Figure S13, Supporting Information) and temperature on enzyme stability (Figure S14, Supporting Information) of mutant W235I were found to be similar to the values determined for the YbfF wild-type.<sup>[5]</sup>

### Kinetic Analysis of Wild-Type and W235I

To establish whether the enhanced enantioselectivity of the mutant W235I is caused by changes in binding affinity and/or turnover rate of the individual enantiomers, kinetic parameters for the enzyme-catalyzed conversion of (*R*)-**1**, (*S*)-**1**, (*R*)-**3** and (*S*)-**3** were determined (Table 2). For substrate **1**, the 2-fold increase in enantioselectivity of the mutant W235I ( $E=20$ ) was due to a  $\sim 6$ -fold increase in catalytic efficiency ( $k_{\text{cat}}/K_{\text{m}}$ ) for (*R*)-**1**, combined with a  $\sim 3$ -fold increase in catalytic efficiency for (*S*)-**1**, when compared to YbfF wild-type ( $E=10$ ). The mutant increased catalytic efficiency for the preferred *R*-enantiomer, was mainly due to a lower  $K_{\text{m}}$ , whereas for the *S*-enantiomer the improvement observed in catalytic efficiency was mainly the result of a higher  $k_{\text{cat}}$ .

For substrate **3**, the results showed that the mutant W235I exhibits slightly lower  $K_{\text{m}}$  values for both

**Table 2.** Steady-state kinetic parameters of wild-type YbfF and mutant W235I for substrate **1** and **3**.<sup>[a]</sup>

Enzyme	Substrate	$K_{\text{m}}$ [mM]	$k_{\text{cat}}$ [ $\text{s}^{-1}$ ]	$k_{\text{cat}}/K_{\text{m}}$ [ $\text{M}^{-1}\text{s}^{-1}$ ]	$E$ <sup>[b]</sup>
WT	( <i>R</i> )- <b>1</b>	$13.6 \pm 4.5$	$62 \pm 10$	4559	10
	( <i>S</i> )- <b>1</b>	$9.7 \pm 0.9$	$4.6 \pm 0.2$	474	
W235I	( <i>R</i> )- <b>1</b>	$2.6 \pm 0.7$	$71.9 \pm 5.6$	27443	16
	( <i>S</i> )- <b>1</b>	$12.9 \pm 2.4$	$21.9 \pm 2$	1695	
WT	( <i>R</i> )- <b>3</b>	$5.8 \pm 1.1$	$15.4 \pm 1.2$	2651	29
	( <i>S</i> )- <b>3</b>	$7.3 \pm 1.2$	$0.66 \pm 0.05$	90	
W235I	( <i>R</i> )- <b>3</b>	$4.7 \pm 0.4$	$113 \pm 3.9$	24042	76
	( <i>S</i> )- <b>3</b>	$4.1 \pm 0.8$	$1.3 \pm 0.1$	317	

<sup>[a]</sup> The steady-state kinetic parameters were determined in 70 mM MOPS buffer (pH 7.5) at 30 °C. Errors represent standard deviations.

<sup>[b]</sup> The enzyme is selective towards the *R*-substrate, producing the *S*-product in large excess.

enantiomers of **3**, when compared to wild-type. However, in terms of  $k_{\text{cat}}$  the mutant W235I showed a  $\sim 7.3$ -fold increase for (*R*)-**3**, whereas for (*S*)-**3** the increase was only  $\sim 2$ -fold. Taken together, these differences in  $K_{\text{m}}$  and  $k_{\text{cat}}$  of mutant W235I are reflected in a  $\sim 9$ -fold increase in the catalytic efficiency for (*R*)-**3** and a  $\sim 3.5$ -fold increase in catalytic efficiency for (*S*)-**3**. This accounts for the observed increase in enantioselectivity of the mutant ( $E=76$ ) when compared to YbF wild-type ( $E=29$ ).

### Characterization of YbF Wild-Type and W235I by Molecular Modeling

In order to unravel differences in activity and enantioselectivity between the best YbF variant and wild-

type YbF, we modeled the *R*- and *S*-enantiomers into the active site of YbF wild-type and the best mutant W235I. Analysis of the most favorable docking poses of YbF revealed striking differences in the positioning of the enantiomeric substrates **1** and **3** into the active site, also with respect to the distance between the  $\text{O}_{\gamma}$  atom of the catalytic nucleophile (Ser-89) and the carbonyl carbon of the substrates (Figure 3). The most favorable poses obtained for (*R*)-**1** reveal that the carbonyl carbon of the substrate is proximal to the  $\text{O}_{\gamma}$  atom of Ser-89 (3.4 Å) for both wild-type YbF and W235I (Figure 3, A). For substrate (*S*)-**1**, the most favorable pose places the carbonyl carbon of the substrate further away from the  $\text{O}_{\gamma}$  atom of Ser-89, with an observed distance of 4.0 Å between the substrate carbonyl carbon and the Ser-89  $\text{O}_{\gamma}$  (Figure 3, B), resulting in a less optimal positioning of

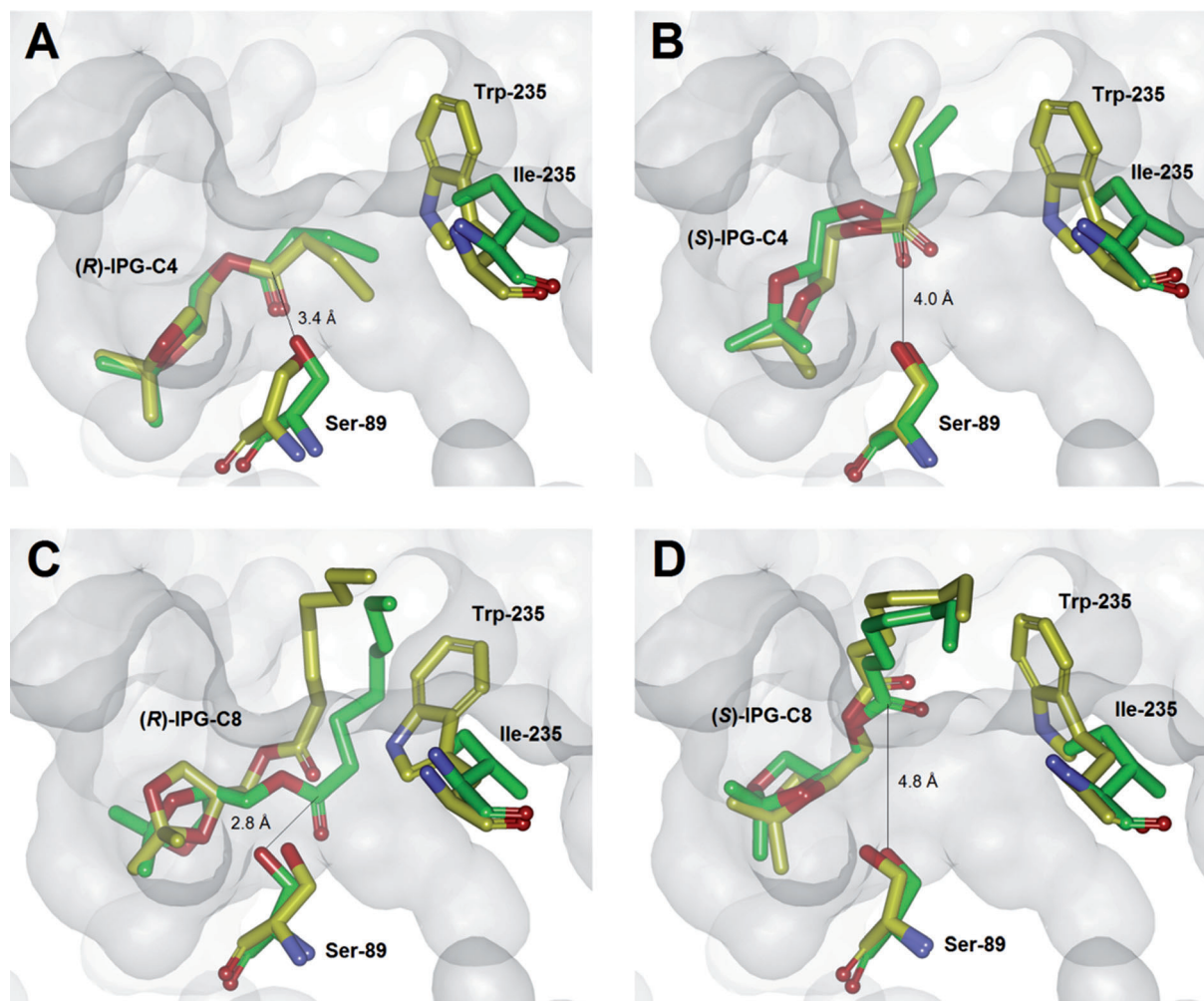


**Figure 3.** Molecular docking of (*R*)-IPG-C4 (*R*-**1**) (A), (*S*)-IPG-C4 (*S*-**1**) (B), (*R*)-IPG-C8 (*R*-**3**) (C) and (*S*)-IPG-C8 (*S*-**3**) (D) into the active site of YbF wild-type (yellow sticks) and mutant YbF W235I (green sticks). The catalytic serine 89 and mutated tryptophan 235 are depicted in yellow and green sticks for YbF wild-type and YbF W235I, respectively. The cavity and crevice of YbF are represented by a grey surface. Depicted are some of the distances (Å) between the catalytic Ser-89  $\text{O}_{\gamma}$  and the carbonyl carbon of the substrate. Docking of substrates and minimization runs were performed using available tools in Discovery Studio 2.5. The figure was generated using Discovery Studio 2.5.

the substrate for nucleophilic attack in both YbF wild-type and W235I. This change in conformation of the substrate in the active site of W235I may partially explain the increased  $k_{\text{cat}}$  observed for (*S*)-**1** (Table 2).

The mutation W235I seems to contribute mostly to an enhanced enantioselectivity towards (*R*)-**3**. In mutant W235I where the Trp-235 is replaced by the smaller side chain aliphatic residue Ile, the docking results show that (*R*)-**3** further sinks in the pocket of YbF, resulting in a distance reduction between the carbonyl carbon of (*R*)-**3** and the Ser-89 O $\gamma$  from 3.5 Å (wild-type) to 2.8 Å (W235I) (Figure 3, C). This re-orientation of (*R*)-**3** in the active site of W235I seems to contribute to the enhanced  $k_{\text{cat}}$  observed experimentally, which is a determinant for the increased enantioselectivity of the mutant W235I when compared to YbF wild-type (Table 2). In contrast, the binding of (*S*)-**3** is less favorable in both active sites of YbF wild-type and W235I, with observed distances between the carbonyl carbon of (*S*)-**3** and the nucleophilic serine O $\gamma$  of 4.9 Å and 4.8 Å for YbF wild-type and W235I, respectively (Figure 3, D).

The increase in enantioselectivity promoted by the mutation W235I was mainly due to the improvement of the enzyme catalytic efficiency towards the preferred enantiomer (*R*-**3**). To the best of our knowledge, the intracellular carboxyl esterase A from *B. coagulans* exhibited the higher enantioselectivity towards IPG caprylate esters reported in literature. Molinari et al. showed that the CesaA from *B. coagulans* hydrolyzed IPG caprylate esters producing (*S*)-IPG with 94% enantiomeric excess at 23% conversion, corresponding to an *E* value of 43.<sup>[15,16]</sup>

Although the YbF selectivity towards substrate **3** is high enough for practical applications, further improvement might still be possible. A plausible approach would pass by promoting a second round of mutagenesis in an iterative manner, according to the iterative saturation mutagenesis approach (ISM) described by Reetz. Another approach would be the selection and mutation of second-sphere residues, residues that are not in direct contact to the substrate but still make part of the enzyme binding pocket.<sup>[17,18,26]</sup>

## Conclusions

In summary, the enantioselectivity of YbF from *E. coli* toward caprylate esters of 1,2-*O*-isopropylidene-glycerol (IPG) could be improved (up to *E* = 77) by a structure-based rational design approach. The best mutant (W235I) has been identified based on molecular docking experiments, followed by the use of a screening assay based on the hydrolytic activities towards the substrate (**1**). The YbF mutant W235I displays higher enantioselectivity in hydrolyses of IPG caprylate esters than the reported *B. coagulans* CesaA

enzyme, which renders the YbF mutant to a very suitable candidate for practical applications in the kinetic resolution of IPG esters.

## Experimental Section

### General

All reagents were of analytical grade unless specified otherwise. (*R*)-IPG butyrate, (*S*)-IPG butyrate, (*R*)-IPG caprylate and (*S*)-IPG caprylate were a kind gift of Dr. Frank Dekker (Department of Pharmaceutical Gene Modulation, University of Groningen, The Netherlands). The sources for the media components, buffers, and molecular biology reagents, including PCR, purification, gel extraction, and Miniprep kits, are reported elsewhere.<sup>[5]</sup> Oligonucleotides for DNA amplification were synthesized by Operon Biotechnologies (Cologne, Germany).

### Plasmids, Bacterial Strains and Media

*E. coli* strain BL21 (DE3) (Stratagene, La Jolla, CA) was used for cloning and isolation of plasmids, and, in combination with the pET26b vector (Novagen), for recombinant protein production. *E. coli* cells were grown in Luria-Bertani (LB) medium containing bactotrypton (8%, w/v), yeast extract (0.5%, w/v) and sodium chloride (0.5%, w/v). When required, kanamycin (Kan; 30  $\mu\text{g mL}^{-1}$ ), Difco agar (15  $\text{g L}^{-1}$ ), and IPTG (1 mM) were added to the medium. DNA sequencing was performed by Macrogen (Seoul, Korea). Recombinant DNA techniques were performed as described by Sambrook et al.<sup>[19]</sup> YbF wild-type and mutants were produced in *E. coli* BL21 (DE3) and purified to homogeneity using a previously published protocol.<sup>[5]</sup>

### Library Construction and Screening

The construction of single-site mutagenesis libraries (NDT) consisting of 12 naturally occurring amino acids<sup>[11]</sup> at positions 25, 124, 185 and 235 in YbF was performed by megaprimer PCR, using pET26bYbFwt as the template, according to Miyazaki et al.<sup>[20]</sup> The resulting plasmids harboring the mutant *ybfF* gene were transformed into electrocompetent BL21 (DE3) cells. Transformants were selected on LB/Kan plates. Colonies were picked with sterile toothpicks into 96-wells plates (flat bottom, Greiner Bio-one) containing LB/Kan medium (200  $\mu\text{L}$  per well). Cells were grown overnight at room temperature with agitation. ZYP-5052 medium<sup>[21]</sup> (1.3 mL) containing kanamycin was then added to the wells and the plates were incubated for 1 day at room temperature, with agitation, to allow protein production. A portion (50  $\mu\text{L}$ ) of each culture was diluted in demi water (150  $\mu\text{L}$ ) and the  $A_{600}$  was determined in a 96-well plate reader (Multiscan accent, Labsystems). The cells of the remaining cultures were harvested by centrifugation (2000  $\times g$ , 4°C, 15 min). The cell pellet was then resuspended in Bug-buster solution (Novagen, Merck, Germany) (300  $\mu\text{L}$ ) and the plates were incubated at room temperature with agitation for 30 min. Subsequently, 200  $\mu\text{L}$  of BES buffer (5 mM, pH 7.2) was added to each well and centrifugation was performed (2000  $\times g$ , 4°C, 1 hour) to remove unbroken cells

and cell debris. Aliquots (20  $\mu\text{L}$ ) of the cell free extracts were transferred into new 96-well plates containing BES buffer (100  $\mu\text{L}$ , 5 mM, pH 7.2), 4-nitrophenol (1 mM, pH 7.2), and IPG butyrate (*R* or *S*) stock solutions of 5 mM. The plate was placed in the microplate reader and shaken for 15 s, the decrease in absorbance at 405 nm was monitored each minute over 30 min, at 30 °C. Cell-free extracts prepared from *E. coli* BL21 (DE3) cells transformed with empty pET26b vector were used as references. Activities were determined from slopes in the linear section of the curve.<sup>[13]</sup> YbF mutants of which the enantioselectivity was potentially increased were selected and purified for further characterization, and the corresponding genes were sequenced.

### Kinetic Resolution of IPG Esters

The procedure for the determination of the enantioselectivity of YbF wild-type and mutants towards IPG esters is reported elsewhere.<sup>[5]</sup> The samples were analyzed by chiral GC on a Hewlett Packard 5890 series II gas chromatograph, as described by Dröge et al.<sup>[22]</sup> The non-enzymatic hydrolysis of the substrates was negligible under the conditions used. The enantiomeric excess (*ee*) of products and substrates was calculated according to Chen et al.<sup>[23]</sup> The calculated values of enantiomeric excess of products and substrates were used to determine the *E*-values by using the program Selectivity (K. Faber, H. Hoenig, ftp://borgc185.kfunigraz.ac.at/pub/enantio/). The chromatographs data corresponding to the kinetic resolution of racemic IPG-caprylate (**3**) with YbF wild-type and mutant W235I are provided as Figure S1 to Figure S12 in the Supporting Information.

### Determination of the Kinetic Parameters

The kinetic parameters  $K_m$  and  $k_{cat}$  were determined using a previously published protocol.<sup>[5]</sup>

### Molecular Docking

Substrates *R*-**1**, *S*-**1**, *R*-**3** and *S*-**3** were constructed and molecular docking simulations were performed in wild-type YbF (Protein Data Bank accession code: 3BF7) and the structural model of the YbF mutant (W235I), using the grid-based approach CDOCKER.<sup>[24,25]</sup> The active site residue W235 of YbF was mutated to isoleucine *in silico*. The mutant enzyme model was energy minimized consisting of 150 steps of steepest descent followed by 500 iterations of the adopted basis-set Newton-Raphson algorithm. All structures containing substrates were further energy minimized using CHARMM, consisting of 5000 steps of steepest descent followed by 5000 iterations of the adopted basis-set Newton-Raphson algorithm using an energy tolerance of 0.01 kcal mol<sup>-1</sup> Å<sup>-1</sup>.

### Acknowledgements

L.F.G. the recipient of an Ubbo Emmius fellowship. G.J.P. was financially supported by VIDI grant 700.56.421 from the Division of Chemical Sciences of the Netherlands Organisation for Scientific Research (NWO-CW). We thank Dr. Frank

Dekker (University of Groningen) for the kind gift of the IPG esters.

### References

- [1] U. T. Bornscheuer, *FEMS Microbiol. Rev.* **2002**, *26*, 73–81.
- [2] D. Bottcher, U. T. Bornscheuer, *Curr. Opin. Microbiol.* **2010**, *13*, 274–282.
- [3] J. Jurczak, S. Pikul, T. Bauer, *Tetrahedron* **1986**, *42*, 447–488.
- [4] E. Maconi, R. Gualandris, F. Aragozzini, *Biotechnol. Lett.* **1990**, *12*, 415–418.
- [5] L. F. Godinho, C. R. Reis, P. G. Tepper, G. J. Poelarends, W. J. Quax, *Appl. Environ. Microbiol.* **2011**, *77*, 6094–6099.
- [6] S. Y. Park, S. H. Lee, J. Lee, K. Nishi, Y. S. Kim, C. H. Jung, J. S. Kim, *J. Mol. Biol.* **2008**, *376*, 1426–1437.
- [7] K. P. Hopfner, E. Kopetzki, G. B. Kresse, W. Bode, R. Huber, R. A. Engh, *Proc. Natl. Acad. Sci. USA* **1998**, *95*, 9813–9818.
- [8] F. H. Arnold, *Nature* **2001**, *409*, 253–257.
- [9] Y. L. Boersma, M. J. Dröge, A. M. van der Sloot, T. Pijning, R. H. Cool, B. W. Dijkstra, W. J. Quax, *Chem-biochem* **2008**, *9*, 1110–1115.
- [10] Y. L. Boersma, M. J. Dröge, W. J. Quax, *FEBS J.* **2007**, *274*, 2181–2195.
- [11] L. G. Otten, F. Hollmann, I. W. Arends, *Trends Biotechnol.* **2010**, *28*, 46–54.
- [12] M. T. Reetz, J. J. Peyralans, A. Maichele, Y. Fu, M. Maywald, *Chem. Commun.* **2006**, *41*, 4318–4320.
- [13] L. E. Janes, A. C. Lowendahl, R. J. Kazlauskas, *Chem. Eur. J.* **1998**, *4*, 2324–2331.
- [14] M. T. Reetz, D. Kahakeaw, R. Lohmer, *ChemBioChem* **2008**, *9*, 1797–1804.
- [15] F. Molinari, O. Brenna, M. Valenti, F. Aragozzini, *Enzyme Microb. Technol.* **1996**, *19*, 551–556.
- [16] D. Romano, F. Falcioni, D. Mora, F. Molinari, A. Buthe, M. Schumacher, *Tetrahedron: Asymmetry* **2005**, *16*, 841–845.
- [17] M. T. Reetz, J. D. Carballeira, *Nat. Protoc.* **2007**, *2*, 891–903.
- [18] M. T. Reetz, *Angew. Chem.* **2011**, *123*, 144–182; *Angew. Chem. Int. Ed.* **2011**, *50*, 138–174.
- [19] J. Sambrook, D. W. Russell, *Molecular cloning: a laboratory manual*, 3<sup>rd</sup> edn., Cold Spring Harbor Laboratory Press, New York, **2001**.
- [20] K. Miyazaki, M. Takenouchi, *Biotechniques* **2002**, *33*, 1033–1038.
- [21] F. W. Studier, *Protein Expres. Purif.* **2005**, *41*, 207–234.
- [22] M. J. Dröge, R. Bos, H. J. Woerdenbag, W. J. Quax, *J. Sep. Sci.* **2003**, *26*, 771–776.
- [23] C. S. Chen, Y. Fujimoto, G. Girdaukas, C. J. Sih, *J. Am. Chem. Soc.* **1982**, *104*, 7294–7299.
- [24] J. A. Erickson, M. Jalaie, D. H. Robertson, R. A. Lewis, M. Vieth, *J. Med. Chem.* **2004**, *47*, 45–55.
- [25] G. S. Wu, D. H. Robertson, C. L. Brooks, M. Vieth, *J. Comput. Chem.* **2003**, *24*, 1549–1562.
- [26] L. G. Otten, W. J. Quax, *Biomol. Eng.* **2005**, *22*, 1–9.